Journal of the Mechanics and Physics of Solids 60 (2012) 319–332

Contents lists available at SciVerse ScienceDirect

Journal of the Mechanics and Physics of Solids

journal homepage: www.elsevier.com/locate/jmps

A theory for large deformation and damage of interpenetrating polymer networks

Xuanhe Zhao *

Soft Active Materials Laboratory, Department of Mechanical Engineering and Materials Science, Duke University, Durham, NC 27708, USA

ARTICLE INFO

Article history:
Received 25 May 2011
Received in revised form
3 September 2011
Accepted 18 October 2011
Available online 25 October 2011

Keywords:
Double-network hydrogels
Mullins effect
Necking instability
Eight-chain model
Network alteration theory

ABSTRACT

Elastomers and gels can be formed by interpenetrating two polymer networks on a molecular scale. This paper develops a theory to characterize the large deformation and damage of interpenetrating polymer networks. The theory integrates an interpenetrating network model with the network alteration theory. The interpenetration of one network stretches polymer chains in the other network and reduces its chain density, significantly affecting the initial modulus, stiffening and damage properties of the resultant elastomers and gels. Double-network hydrogels, a special type of interpenetrating polymer network, have demonstrated intriguing mechanical properties including high fracture toughness, Mullins effects, and necking instability. These properties have been qualitatively attributed to the damage of polymer networks. Using the theory, we quantitatively illustrate how the interplay between polymer-chain stiffening and damage-induced softening can cause the Mullins effect and necking instability. The theory is further implemented into a finite-element model to simulate the initiation and propagation of necking instability in double-network hydrogels. The theoretical and numerical results are compared with experimental data from multiple cyclic compressive and tensile tests.

1. Introduction

An interpenetrating polymer network (IPN) consists of two or more polymer networks, at least one of which is polymerized and/or crosslinked in the immediate presence of the other(s) (Sperling and Mishra, 1996). As illustrated in Fig. 1(a), the polymer networks are interlaced on a molecular scale but not covalently bonded to each other. Above glass transition temperatures, IPNs are generally capable of large deformation and they are referred to as IPN elastomers. The IPNs can also imbibe a large amount of solvents to swell into IPN gels. If water is used as the solvent, the resultant gels are called IPN hydrogels.

Interpenetrating polymer networks have found important applications in diverse technologies, including organic solar cells (Halls et al., 1995; Ma et al., 2005), drug delivery (Risbud et al., 2000), tissue engineering(Gong et al., 2003), polymer actuators (Ha et al., 2006; Zhao and Suo, 2010), and energy harvesters (Brochu et al., 2009; Koh et al., 2009). Many of these applications rely on the unique mechanical properties of IPNs. For example, the IPN dielectric elastomer developed by Ha et al. (2006) can achieve over 300% voltage-induced strain without prestretch, while the actuation strain of unprestretched common elastomers is less than 40% (Zhao and Suo, 2007). It has been shown that the giant actuation strain of IPN

* Tel.: +1 919 660 5441.
E-mail address: xz69@duke.edu

0022-5096/$ - see front matter © 2011 Elsevier Ltd. All rights reserved.
doi:10.1016/j.jmps.2011.10.005

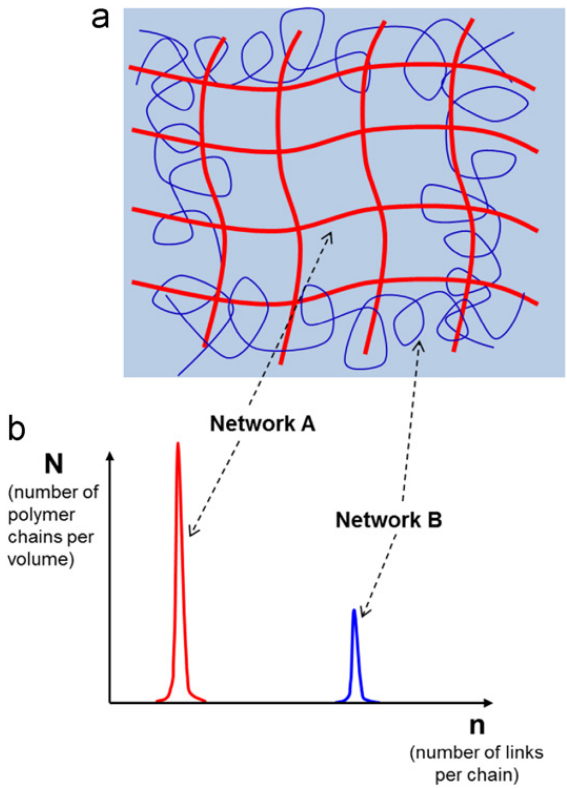

Fig. 1. Schematics of an interpenetrating polymer network (a) and the distribution of the chain densities and chain lengths of two networks (b).

dielectric elastomers is due to their low moduli at small deformation but steep stiffening at moderate deformation (Zhao and Suo, 2010). Constitutive models of IPN dielectric elastomers have also been developed to design polymers for actuators and energy harvesters (Goulbourne, 2011; Suo and Zhu, 2009). As another example, Gong et al. (2003) used two polymer networks with distinctly different chain lengths to form a particular type of IPN hydrogels. This so-called double-network hydrogels can reach fracture energy over 1000 J m^{-2} despite about 90% water content of the hydrogel (Nakajima et al., 2009; Tanaka et al., 2005). This value exceeds the fracture energy of rubber at low crack velocities, which is in distinct contrast to the fragile nature of common hydrogels. The anomalous high toughness of the double-network hydrogels has made them a promising scaffold for regenerating load-bearing tissues (Yasuda et al., 2009) and for delivering drugs (Risbud et al., 2000).

These applications aside, understanding the mechanical properties of IPNs is a fundamental and challenging topic in polymer mechanics and physics. Although intensive studies on IPNs have been carried out, many intriguing phenomena related to the mechanics of IPNs are still not well understood. For example, the high toughness of double-network hydrogels has been attributed to stretch-induced softening or Mullins effect of the hydrogels (Brown, 2007; Tanaka, 2007), a mechanism analogous to the transformation-toughening in brittle materials (see e.g. McMeeking and Evans, 1982). The Mullins effect of double-network hydrogels as illustrated in Fig. 2(b) has been qualitatively attributed to the damage of polymer networks (Webber et al., 2007; Yu et al., 2009). However, it is still not clear how to quantitatively relate the large deformation and damage to the characters of the polymer networks such as polymer-chain lengths and densities. In addition, necking instability as illustrated in Fig. 2(b) has been observed in tensile tests of some double-network hydrogels (Na et al., 2006) but not others (Webber et al., 2007). The exact mechanism that causes this difference is still not well understood.

The aim of this work is to develop a mechanistically motivated model that is capable of explaining various mechanical phenomena of IPN elastomers and gels under large deformation. The model will adapt the classical network model (see e.g. Arruda and Boyce, 1993) into an interpenetrating network model. The model will further implement the network alteration theory (Marckmann et al., 2002) to characterize the damage of the IPNs under deformation. With the model, we will quantitatively show that the interpenetration of one network stretches polymer chains in the other network and reduces its chain density, significantly affecting the initial modulus, stiffening and damage properties of the resultant IPNs. The characters of stiffening and subsequent damage of one network determine the special Mullins effect of double-network hydrogels. The necking instability of double-network hydrogels requires both the damage-induced softening of one network and the stiffening of the other network.

The plan of the paper is as follow. Section 2 presents the constitutive equations for the large deformation and damage of IPNs. In Section 3, we discuss the effect of interpenetration of other networks on the mechanical properties of IPNs. We further compare the theoretical results with experimental data from cyclic compressive and tensile tests of double-network

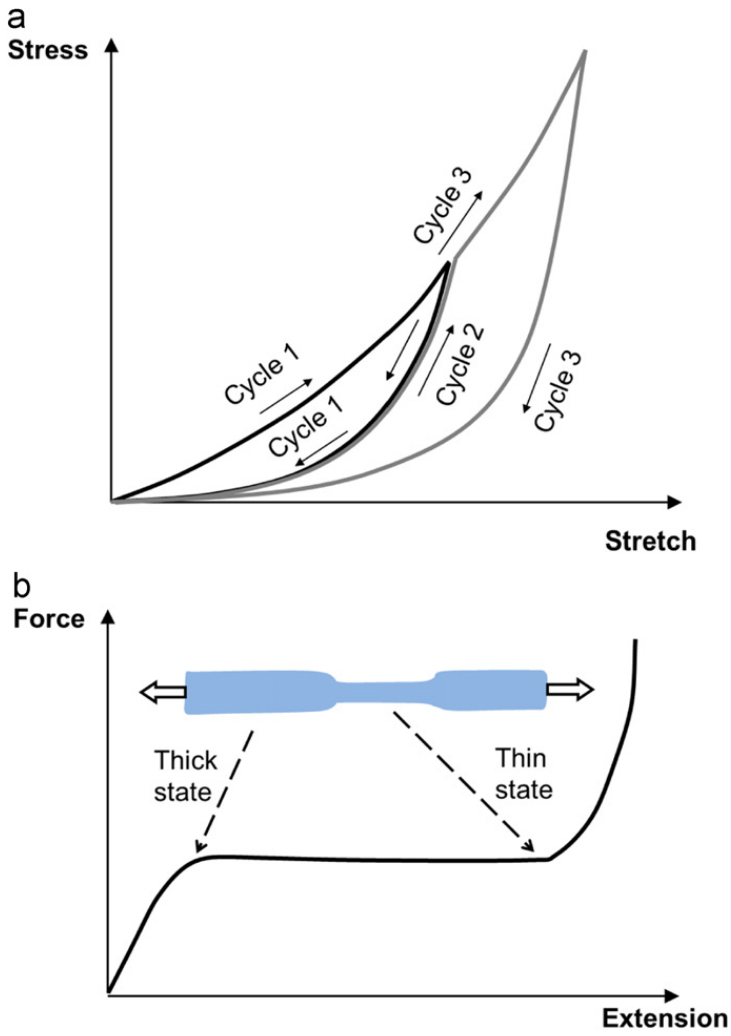

Fig. 2. Double-network hydrogels, a type of interpenetrating polymer network, can give Mullins effect (a) and necking instability (b) under deformation.

hydrogels (Webber et al., 2007). Section 4 discusses the necking instability experimentally observed in double-network hydrogels (Na et al., 2006). The theory is further implemented into a finite-element model to simulate the initiation and propagation of the necking instability. Section 5 gives the conclusive remarks of the paper.

2. Constitutive model of interpenetrating polymer networks

2.1. Free energy function

In thermodynamic systems, the constitutive properties of hyperelastic materials are given by their free energy functions. The free energy of an IPN comes from two molecular processes: (1) stretching polymer chains in the polymer networks that constitute the IPN, and (2) mixing polymers of different networks and, in the case of an IPN gel, solvent molecules (Flory and Rehner, 1943b; Hong et al., 2008). Following Flory and Rehner (1943b), the free energy function of an IPN composed of m networks takes the form

$$W = \sum_{i=1}^{m} W_i^S + W^M \tag{1}$$

where W_i^S is the free energy due to stretching the ith network per unit volume of the IPN, and W^M is the free energy due to mixing polymers and solvents per unit volume of the IPN.

The free energy of mixing depends on the concentrations of different constituents of the IPN. Over the time scale of deforming IPN elastomers and gels, the variation of polymer and solvent concentrations have been observed to be negligible (see e.g. Gong et al., 2003; Ha et al., 2006; Na et al., 2006; Tanaka et al., 2005; Webber et al., 2007). This paper aims to explain experimental phenomena of IPNs that do not involve concentration variation during deformation, so W^M is assumed to be constant in Eq. (1). The IPNs are further taken to be incompressible, as their bulk moduli are much higher

than shear moduli. Therefore, the principal stresses of the IPN can be calculated as

$$\sigma_1 = \sum_{i=1}^{m} \lambda_1 \frac{\partial W_i^S}{\partial \lambda_1} - P \tag{2a}$$

$$\sigma_2 = \sum_{i=1}^{m} \lambda_2 \frac{\partial W_i^S}{\partial \lambda_2} - P \tag{2b}$$

$$\sigma_3 = \sum_{i=1}^{m} \lambda_3 \frac{\partial W_i^S}{\partial \lambda_3} - P \tag{2c}$$

where λ_1, λ_2, and λ_3 are the principal stretches of the IPN, and P the hydrostatic pressure that can be determined from boundary conditions.

2.2. Interpenetrating eight-chain network model

The free energy function for stretching polymer networks can be characterized by either phenomenological models or network models (see e.g. a recent review by Boyce and Arruda, 2000). In order to relate the physical (microscopic) structures of IPNs to their deformation mechanism, we choose to follow the network-model approach to construct the free energy function of IPNs. Polymer networks of the IPNs are considered as crosslinked networks of freely joint chains (Rubinstein and Colby, 2003). The average unstretched length of a chain of the ith network is $\sqrt{n_i}l_i$, where n_i is the number of freely joint links on a chain of the ith network, and l_i the length of the link. The stretch of a polymer chain of the ith network can be calculated as $\Lambda_i = r_i/\sqrt{n_i}l_i$, where r_i is the stretched length of the chain. The chain has a full extension length of $n_i l_i$ so that the stretch limit of the chain is $\sqrt{n_i}$. The effect of the stretch limit on the stretch–stress behavior of IPNs is captured by Langevin statistics (Kuhn and Grun, 1942), and the free energy of the chain can be expressed as

$$w_i = n_i kT\left(\frac{\beta_i}{\tanh\beta_i} + \log\frac{\beta_i}{\sinh\beta_i}\right) \tag{3}$$

where $\beta_i = L^{-1}(\Lambda_i/\sqrt{n_i})$ and L^{-1} is the inverse Langevin function defined by $L(x) = \coth(x) - 1/x$.

In fabricating IPNs, if any crosslinked polymer network swells homogeneously and isotropically in monomers (or polymer solutions) of networks to be polymerized (or crosslinked), the elasticity of the crosslinked network will not change significantly before and after other networks' polymerization (or crosslinking). In this case, we can assume any polymer network of an IPN is swollen in monomers (or polymer solutions) of others, when considering the contribution of this network to the free energy of the IPN as illustrated in Fig. 3. Therefore, the elasticity of one polymer network will be

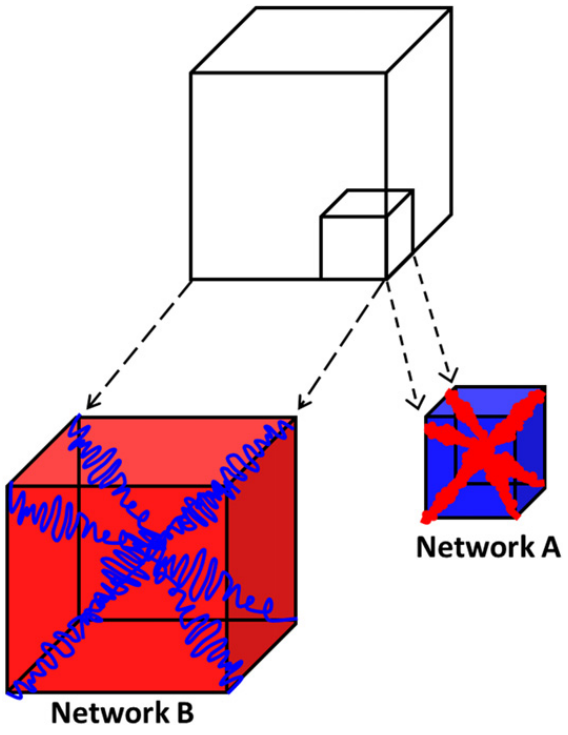

Fig. 3. Schematics of the interpenetrating eight-chain network model. The interpenetration of one network stretches polymer chains in the other network and reduces its chain density.

affected in two ways by the interpenetration of other networks: (1) to stretch polymer chains isotropically and homogeneously without externally applied forces, and (2) to decrease the density of polymer chains, i.e.

$$\Lambda_i = C_i^{-1/3}\Lambda_i' \tag{4a}$$

$$N_i = \frac{N_i'}{C_i} \tag{4b}$$

where C_i is the volume concentration of the ith network in the IPN, Λ_i' is the stretch of a chain of the ith network due to the IPN's deformation, N_i' is the number of chains of the ith network per unit volume of the IPN, and N_i is the number of chains of the ith network per unit volume of the ith network (without others).

A network model is needed to relate the deformation of an IPN to the stretches of polymer chains (see e.g. Arruda and Boyce, 1993; Flory and Rehner, 1943a; Treloar and Riding, 1979; Wang and Guth, 1952). We choose the eight-chain network model developed by Arruda and Boyce (1993) due to its simple mathematical expression and its ability to characterize various deformation modes with only two parameters. As illustrated in Fig. 3, a unit cube from a network of the IPN has eight chains along the half diagonals of the cube. Unit cubes of different networks are overlapped to form the IPN (Fig. 3). As the IPN is deformed, the chains of the same network are stretched by the same ratio. Considering Eq. (4a), the stretch of a chain on the ith network of the IPN can be calculated as

$$\Lambda_i = C_i^{-1/3}\sqrt{\frac{\lambda_1^2+\lambda_2^2+\lambda_3^2}{3}} \tag{5}$$

The stretch consists of two parts: $C_i^{-1/3}$ due to the interpenetration of other networks and solvent, and $\sqrt{(\lambda_1^2+\lambda_2^2+\lambda_3^2)/3}$ due to the deformation of the IPN. Although the deformation-induced stretch is the same for all networks, the total stretches for different networks can be different, since the interpenetration-induced stretches depend on the concentrations of networks.

Considering Eqs. (3)–(5), the free energy from stretching the *ith* polymer networks per unit volume of the IPN can be calculated as (Boyce and Arruda, 2001)

$$W_i^S = C_i N_i n_i kT\left(\frac{\beta_i}{\tanh\beta_i}+\log\frac{\beta_i}{\sinh\beta_i}\right) \tag{6}$$

By substituting Eq. (6) into Eq. (2), we can calculate the principal stresses of the IPN as

$$\sigma_1 = \sum_{i=1}^{m}\frac{C_i^{1/3}N_i\sqrt{n_i}kT\beta_i}{3\Lambda_i}\lambda_1^2 - P \tag{7a}$$

$$\sigma_2 = \sum_{i=1}^{m}\frac{C_i^{1/3}N_i\sqrt{n_i}kT\beta_i}{3\Lambda_i}\lambda_2^2 - P \tag{7b}$$

$$\sigma_3 = \sum_{i=1}^{m}\frac{C_i^{1/3}N_i\sqrt{n_i}kT\beta_i}{3\Lambda_i}\lambda_3^2 - P \tag{7c}$$

The stress in Eq. (7) accounts for the contributions from stretching polymer chains in all networks of an IPN under deformation. It should be noted that the stress in Eq. (7) is not equal to a summation or average of stresses in single-network polymers arranged in parallel, because the interpenetration of one network reduces polymer-chain densities of other networks in an IPN and also stretches polymer chains in other networks without externally applied forces.

For uniaxial tension or compression of an IPN, the stress can be calculated as

$$\sigma = \sum_{i=1}^{m}\frac{C_i^{1/3}N_i\sqrt{n_i}kT\beta_i}{3\Lambda_i}\left(\lambda^2-\frac{1}{\lambda}\right) \tag{8}$$

where λ is the stretch in tension or compression.

2.3. Alteration of interpenetrating polymer networks

Stretch-induced softening or Mullins effect has been widely observed in elastomers, especially in filled rubbers. A variety of theories and models have been developed for the phenomena, including damage theories (Blanchard and Parkinson, 1952; Govindjee and Simo, 1991; Lion, 1996), domain-evolution theories (Johnson and Beatty, 1993; Mullins and Tobin, 1965; Qi and Boyce, 2004), phenomenological theories (Dorfmann and Ogden, 2003; Miehe, 1995), micro-mechanics models (Bergstrom and Boyce, 1999), and network alteration theory (Marckmann et al., 2002).

Recently, Mullins effect and large-strain hysteresis have been observed in deforming double-network hydrogels, a special type of IPN (Gong et al., 2003; Nakajima et al., 2009; Webber et al., 2007). The Mullins effect of double-network hydrogels is substantially different from that of filled rubbers in that (Webber et al., 2007) (1) the deformed hydrogels have no substantial recovery of their virgin behaviors when the hydrogels are left to rest without stress; (2) the hysteresis

of the hydrogels in the second cycle is negligible, if the deformation of the second cycle is smaller than the maximum deformation of the first cycle, as illustrated in Fig. 2(a); and (3) the hysteretic dissipation has negligible dependence on deformation rate, implying that there is negligible viscous dissipation (Gong et al., 2003; Webber et al., 2007).

The Mullins effect of double-network hydrogels has been qualitatively attributed to the breaking of polymer chains and crosslinks in the shorter-chain network under deformation (Webber et al., 2007; Yu et al., 2009). We implement the network alteration theory (Marckmann et al., 2002) into the shorter-chain networks of the hydrogels to characterize the Mullins effect. The physical picture of the model is illustrated in Fig. 4. A hydrogel with two networks is under deformation. As the shorter-chain network is stretched close to its extension limit, the chains and crosslinks in the network break (Lake and Thomas, 1967). As a result, some of the chains become inactive terminal chains that do not contribute to the elasticity of the network, while other chains rearrange into longer chains with higher number of links, as illustrated in Fig. 4(b). The formation of longer chains is more significant in physically crosslinked networks than in chemically crosslinked networks (An et al., 2010; Sun et al., 2011).

To capture the above physical picture, the chain length and density of the shorter-chain network (i.e. network A) are expressed as functions of the maximum stretch of the chains (Marckmann et al., 2002), i.e.

$$N_A = N_A(\Lambda_A^{max}) \tag{9a}$$

$$n_A = n_A(\Lambda_A^{max}) \tag{9b}$$

where the maximum stretch $\Lambda_A^{max} = \max_{0 \le \tau \le t} [\Lambda_A(\tau)]$, and t is the current time in the deformation process. The parameter Λ_A^{max} can be regarded as an internal variable for the free energy function W, and the thermodynamic inequality requires

$$\frac{\partial W}{\partial \Lambda_A^{max}} \delta \Lambda_A^{max} \le 0 \tag{10}$$

where $\delta\Lambda_A^{max}$ is an infinitesimal increase of Λ_A^{max}. Following Chagnon et al. (2006), Eqs. (9a) and (9b) can be taken as exponential functions:

$$N_A = N_{A0} \exp[-p(\Lambda_A^{max} - C_A^{-1/3})] \tag{11a}$$

$$n_A = n_{A0} \exp[q(\Lambda_A^{max} - C_A^{-1/3})] \tag{11b}$$

where n_{A0} and N_{A0} are the link number per chain and chain density in the undeformed shorter-chain network, and p and q are material parameters to characterize the decrease of chain density and increase of chain length. The network-alteration process and Eq. (10) require $p \ge q \ge 0$. In one extreme case, if $p = q > 0$, we have $N_A n_A$ maintains constant, so no inactive terminal chain forms during deformation. In another extreme case, if $p > q = 0$, we have n_A maintains constant, which means the chain length in the shorter-chain network does not change during deformation.

Substituting Eqs. (11a), (11b) into Eq. (8), and considering $n_{A0} N_{A0} \nu_A = 1$ and $n_B N_B \nu_B = 1$ for volume conservation, we have the stress for uniaxial tension or compression as

$$\sigma = \left(\frac{C_A^{1/3} kT \beta_A}{3\nu_A \sqrt{n_{A0}} \Lambda_A} \exp\left[\left(\frac{1}{2} q - p \right) (\Lambda_A^{max} - C_A^{-1/3}) \right] + \frac{C_B^{1/3} kT \beta_B}{3\nu_B \sqrt{n_B} \Lambda_B} \right) \left(\lambda^2 - \frac{1}{\lambda} \right) \tag{12}$$

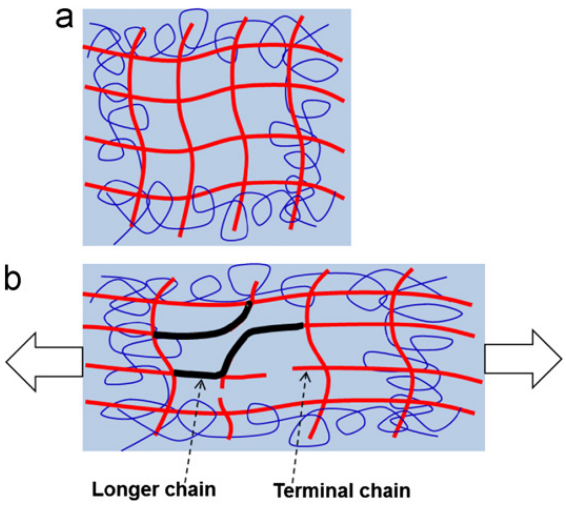

Fig. 4. Schematics of the breaking of chains and crosslinks in the shorter-chain network.

where v_A and v_B are the volumes of single links in network A and B, respectively. For simplicity, assuming $v=v_A=v_B$, the stress of Eq. (12) can be normalized as

$$\frac{v\sigma}{kT}=\left(\frac{C_A^{1/3}\beta_A}{3\sqrt{n_{A0}}\Lambda_A}\exp\left[\left(\frac{1}{2}q-p\right)(\Lambda_A^{max}-C_A^{-1/3})\right]+\frac{C_B^{1/3}\beta_B}{3\sqrt{n_B}\Lambda_B}\right)\left(\lambda^2-\frac{1}{\lambda}\right) \tag{13}$$

3. Large deformation and damage of interpenetrating polymer networks

3.1. Initial modulus and stiffening

The mechanical property of an IPN greatly depends on the distribution of polymer-chain lengths (i.e. n_i) and chain densities (i.e. N_i). In IPN elastomers and gels, the difference in chain lengths of different networks is usually set to be very large (Gong et al., 2003; Ha et al., 2006; Nakajima et al., 2009). Thus, an IPN with two networks A and B usually has a bimodal distribution of chain lengths, such that one network has a higher density of shorter chains, while the other has a lower density of longer chains, i.e. $n_{A0}\ll n_B$ and $N_{A0}\gg N_B$ as illustrated in Fig. 1(b).

Let us first consider an IPN composed of two networks that have no alteration of either network during deformation, i.e. $p=q=0$ in Eq. (13). Considering the chain length distribution as shown in Fig. 1(b), we take $n_{A0}=50$ and $n_B=1000$. The stretch–stress relations for such an IPN are plotted in Fig. 5. For an IPN elastomer (i.e. $C_A+C_B=1$), as the concentration of polymer network with longer chain increases, the initial modulus of the IPN decreases while the stiffening of the IPN is accelerated (Fig. 5(a)). In the case of an IPN gel (i.e. $C_A+C_B<1$), increasing the solvent concentration has a similar effect as increasing the concentration of longer-chain network (Fig. 5(b)). This phenomenon can be understood as follow. An IPN with higher concentration of the shorter-chain network has a higher chain density, and thus a higher initial modulus. On the other hand, a higher concentration of the longer-chain network and solvent can stretch the chains in the shorter-chain network closer to the extension limit, and thus accelerates the stiffening. Therefore, the initial modulus and stiffening property of an IPN can be tuned by varying polymer concentrations and chain lengths of different networks in the IPN.

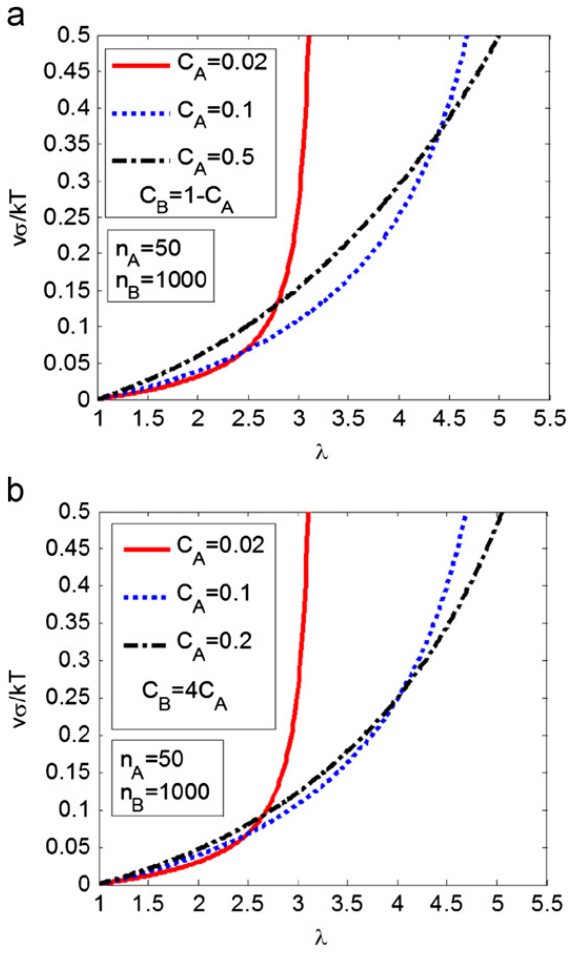

Fig. 5. Stress–stretch curves of IPN elastomers with various polymer ratios (a) and IPN gels with various solvent concentrations (b).

The mechanical properties of bimodal elastomers have been studied by Berry et al. (1956), Flory (1960) and more recently by Mark (1999) and von Lockette et al. (2002). However, these elastomers usually have the long and short chains crosslinked into the same network, and they are assumed to be connected in serial arrangements in the models (von Lockette et al., 2002). On the other hand, the long and short chains in IPNs are not covalently bonded to each other, and they are arranged in an interpenetrating way in our model as illustrated in Fig. 3.

3.2. Alteration of the shorter-chain network

The breaking of polymer chains in the shorter-chain network gives the Mullins effect of double-network hydrogels (Webber et al., 2007). In this section, we will discuss the Mullins effect through the alteration of the shorter-chain network. We set $C_A=0.02$, $C_B=0.08$, $n_{A0}=50$, and $n_B=1000$, and plot the stress–stretch relations for various values of p and q in Fig. 6. If $q=0$, the chain length of the shorter-chain network does not change, while the chain density decreases during deformation. As shown in Fig. 6(a), the double-network hydrogels with different values of p all stiffen around the same stretch limit. Moreover, as the value of p increases, the size of the hysteresis loops in stress–strain curves increases, because a higher value of p gives more inactive terminal chains under the same deformation. On the other hand, if $q=p$, all the chains in the shorter-chain network transform into active longer chains during deformation. The extension limit of the network and the hysteresis both increase with p, as shown in Fig. 6(b).

In Fig. 7(a), we plot the stress–stretch curve of a double-network hydrogel under multiple cycles of loading and unloading. It can be seen that the deformed hydrogel does not recover its virgin behavior and that the hysteresis in cycle 3 is negligible because the stretch in cycle 3 is smaller than the maximum stretch of cycle 2. These characters are consistent with the experimental observations of the Mullins effect in double-network hydrogels (Webber et al., 2007).

Next, we set $C_A=0.08$, $C_B=0.02$, $n_{A0}=50$, $n_B=1000$, and $p=q=0.15$ to model a new double-network hydrogel with the same water concentration and network alteration parameters but different volume ratios of the two networks. The stress–stretch curve of the new hydrogel is plotted in Fig. 7(b). It can be seen that the initial modulus of the new hydrogel is higher than that of the previous one, because the shorter-chain network of the new hydrogel has a higher chain density. However, the hysteresis loop of the new hydrogel becomes smaller than that of the previous one, because of the reduction of the interpenetration-induced stretch in the shorter-chain network. Therefore, the concentrations of the longer-chain network and solvent can significantly affect the stress and hysteresis of the resultant hydrogels, since they affect the interpenetration-induced stretch of the shorter-chain network. On the other hand, the chain length and crosslink density of the longer-chain network do not significantly influence the stress and hysteresis, because the shorter-chain network carries most of the load and undergoes damage.

3.3. Comparison with experimental results of double-network hydrogels

Webber et al. (2007) carried out a series of cyclic uniaxial compressive and tensile tests on the double-network hydrogel invented by Gong et al. (2003). Multiple sets of the nomial stress-stretch data from Webber et al.'s experiments

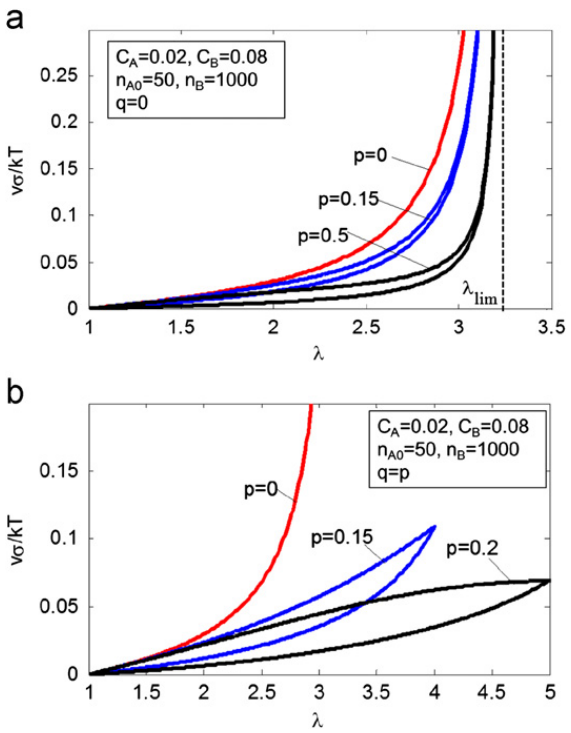

Fig. 6. Mullins effect in double-network hydrogels with $q=0$ (a) and $q=p$ (b).

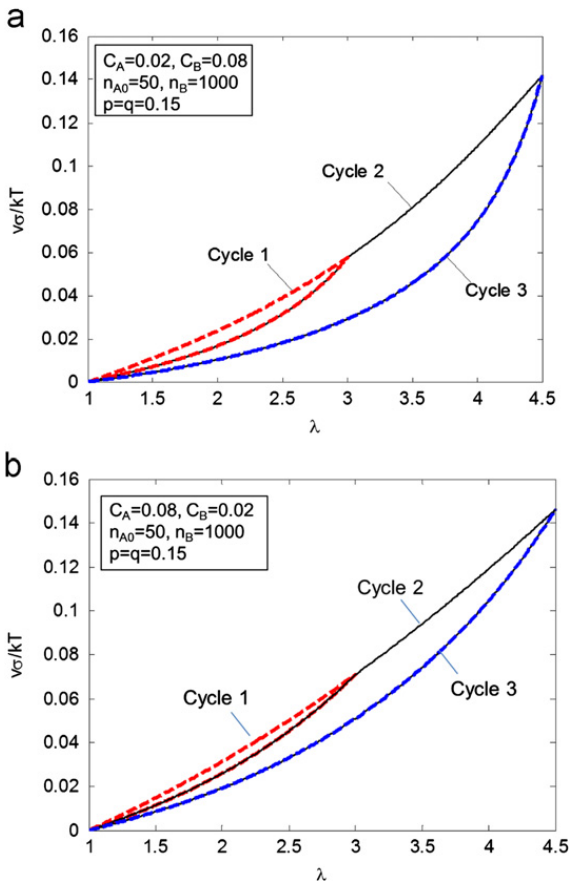

Fig. 7. Mullins effect in double-network hydrogels under multiple loading–unloading cycles, and the effect of interpenetration on the stress-stretch hysteresis.

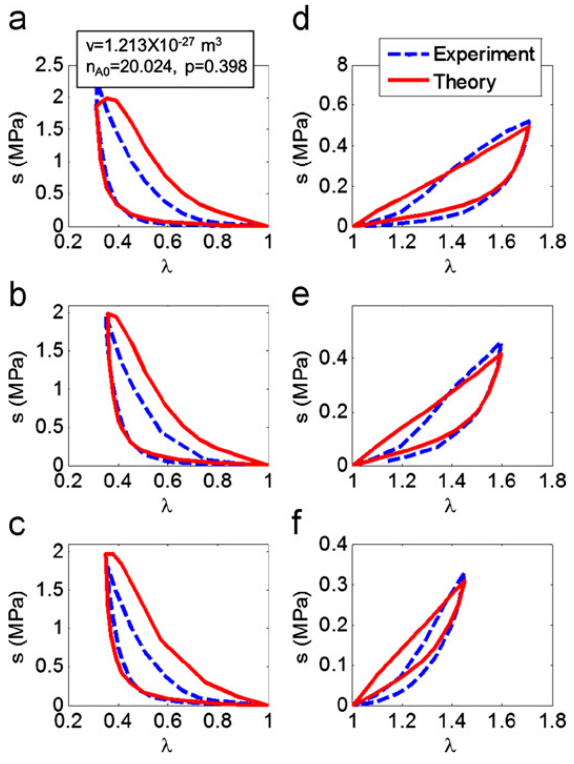

Fig. 8. Comparison of experimental (Webber et al., 2007) and theoretical stress-stretch curves for double-network hydrogels under one cycle of compression (a–c) and tension (d–f).

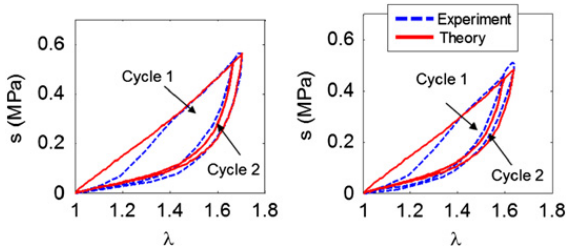

Fig. 9. Comparison of experimental (Webber et al., 2007) and theoretical stress-stretch curves for double-network hydrogels under two cycles of tension.

are plotted in Figs. 8 and 9. In this section, we will compare the experimental results on deformation and Mullins effect with our model's prediction using a minimum amount of fitting parameters. The volume concentration of the two networks in the hydrogels used in Webber et al.'s tests are $C_A=0.013$ and $C_B=0.087$. We further set $n_B=20n_{A0}$, since the chain length of the longer-chain network does not significantly affect the stress and hysteresis of the hydrogel. In addition, Marckmann et al. (2002) and Chagnon et al. (2006) noted that the values of p and q are generally close to each other in the network alteration theory for Mullins effect. Therefore, we further set $p=q$ in our model. Based on Eq. (13) and the above consideration, the nominal stress of the double-network hydrogel under uniaxial tension or compression can be expressed as

$$s=\frac{kT}{\nu}\left(\frac{C_A^{1/3}\beta_A}{3\sqrt{n_{A0}}\Lambda_A}\exp\left[-\frac{1}{2}p(\Lambda_A^{max}-C_A^{-1/3})\right]+\frac{C_B^{1/3}\beta_B}{3\sqrt{n_B}\Lambda_B}\right)\left(\lambda-\frac{1}{\lambda^2}\right) \tag{14}$$

There are three fitting parameters in Eq. (14): ν accounts for the initial modulus of the hydrogel, n_{A0} for the stiffening character, and p for the alteration of the network. The reasonable ranges for these parameters are $10^{-26}\,\mathrm{m}\geq\nu\geq10^{-28}\,\mathrm{m}$, $n_{A0}>1$ and $p\geq0$. The parameters are allowed to vary in these ranges to minimize the difference between experimental and theoretical stresses, using the least-square method. This gives the fitted parameters $\nu=1.213\times10^{-27}\,\mathrm{m}^{-3}$, $n_{A0}=20.024$, and $p=0.3698$. With the fitted parameters, we plot the nominal stress-stretch curves to compare with experimental data. From Figs. 8 and 9, it can be seen that the theoretical results match relatively well with the experimental data from single and multiple cycles of tensile tests. However, the model overestimates the stress-stretch hysteresis from the compressive tests. The inconsistence may be due to the simple network-alteration function, Eq. (11), employed here. To improve the consistency between the model's prediction and experimental results, more fitting parameters may be used to characterize the initial modulus, stiffening, and network alteration of the hydrogel (see e.g. Chagnon et al., 2006). Since the current paper is focused on the physical ideas of the model, we choose to use the minimum amount of fitting parameters.

4. Necking instability

4.1. Stiffening and softening of interpenetrating networks

Initiation and propagation of necking instability has been observed by Na et al. (2006) in stretching a bar of a double-network hydrogel, as illustrated in Fig. 2(b). However, using another double-network hydrogel with similar concentrations of the same polymers but higher crosslink densities, Webber et al. (2007) cannot observe the necking instability during tensile tests.

We propose the following physical picture to explain the phenomena. Under deformation, the chains in the shorter-chain network are first stretched close to their extension limit, which gives the stiffening of the hydrogel. Meanwhile, breaking of chains and crosslinks in the shorter-chain network softens the hydrogel. If the stiffening effect dominates over the softening effect, the stress in the hydrogel will increase drastly when the extension limit is approached, and the high stress may cause fracture of the hydrogel before necking. If the softening effect dominates over the stiffening effect at relative low stresses, the necking instability can set in before the hydrogel fractures.

After the necking instability, if the bar is further deformed, polymer chains in the longer-chain network can be streched close to their extension limit and the double-network hydrogel stiffens again. As a result, the necking stablizes at a thin region of the bar with a higher stretch, as illustrated in Fig. 2(b). Under further deformation, the thin region propagates with consumption of the thick region.

4.2. Effects of material parameters

The material parameters of the double-network hydrogel in Webber et al.'s tests (2007) are given in Section 3.3, i.e. $C_A=0.013$, $C_B=0.087$, $\nu=1.213\times10^{-27}\,\mathrm{m}^{-3}$, $n_{A0}=20.024$, $p=q=0.3698$, and $n_B=20n_{A0}$. In Fig. 10(a), we plot the nominal stress-stretch curve using Eq. (14) with these parameters. It can be seen that the stiffening effect maintains dominant at

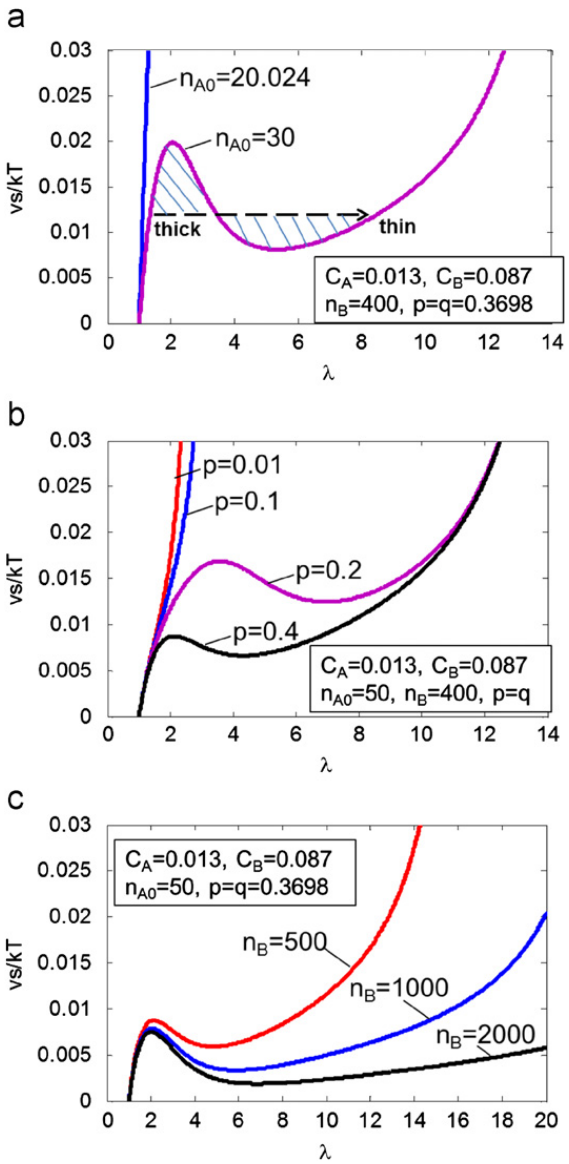

Fig. 10. The effects of shorter-chain length (a), network alteration parameter (b), and longer-chain length (c) on the necking instability of double-network hydrogels.

a relatively high stress. Therefore, Webber et al. (2007) observed the fracture of their IPNs before the necking instability. On the other hand, for IPNs with lower crosslink densities and thus longer chain lengths (e.g. $n_{A0}=30$ in Fig. 10(b)), the softening effect becomes dominant at relative low stresses, where peaks appear on the nominal stress-stretch curves, and thus the necking instability sets in. Further, with the stiffening of the longer-chain network, the bar of the hydrogel stabilizes at a thin region, as shown in Figs. 2(b) and 10(a). The theoretical results are consistent with the fact that Na et al. (2006) observed the necking instability in a double-network hydrogel with a lower crosslink density of the shorter-chain network (i.e. higher n_{A0}) than that of Webber et al.'s hydrogel. In addition, the nominal stress for the transition from the thick state to the thin state can be calculated following the approach used in deformation theory of metal plasticity (Fleck et al., 1994; Hutchinson and Neale, 1981). If no unloading is involved during the transition, the hydrogel can be treated as a reversible hyperplastic material with the same stress-stretch behavior (Wang and Hong, 2011). According to Maxwell's rule in phase transition, the nominal stress for the transition can be calculated by equating the two shaded areas on the curve for $n_{A0}=30$ in Fig. 10(a). Similar transition of states occurs in instability of structures, such as the propagation of buckles along a pipe (Chater and Hutchinson, 1984) and coexistent states in dielectric elastomers (Zhao et al., 2007).

If we keep the chain length of the shorter-chain network (n_{A0}) to be constant, the necking instability can also be tuned by varying the network-alteration parameter, p. A higher value of p can give a dominant softening effect at lower stress and stretch, and thus give the necking instability as shown in Fig. 10(b). Physically, the value of p may be varied by changing the way how a network is crosslinked. A physically crosslinked network usually has a larger value of p than a chemically crosslinked network, because physical crosslinks are generally weaker than covalent bonds (An et al., 2010; Sun et al., 2011).

In addition, by varying the chain length of the longer-chain network (n_B), the stretch of the thin region in the double-network hydrogel can be varied, as shown in Fig. 10(c). This is because n_B determines the extension limit of the longer-chain network, and thus determines the stretch of the thin region in the hydrogel.

4.3. Numerical simulation of the neck instability

In order to further illustrate the physical ideas of the necking instability in double-network hydrogels, we implement the interpenetrating network model with network alteration into finite element software, ABAQUS, with the user subroutine, UHYPER. A bar of the hydrogel is modeled with rectangular axisymmetric elements as shown in Fig. 11(a). The material parameters are taken to be $C_A=0.02$, $C_B=0.08$, $n_{A0}=8$, $n_B=16$, and $p=q=0.8$. The bar undergoes uniaxial tension through prescribed displacements on one end of the bar, as illustrated in Fig. 11(a). We define the effective stretch of the bar as l/L, where l and L are the lengths of the bar at deformed and undeformed states, respectively.

From Fig. 11(a), it can be seen that the bar initially undergoes uniform deformation, when $l/L<1.5$. As the effective stretch further increases, the necking instability sets in, with a thin region initiating around one end of the bar. The initiation of the instability gives a sudden decrease of the nominal stress in the hydrogel bar as shown in Fig. 11(b). The sudden decrease of the nominal stress is corresponding to the transition of the bar from a homogeneous metastable state (e.g. $l/L=1.5$) to an inhomogeneous stable state (e.g. $l/L=1.51$). This is consistent with the experimental observation of reduced nominal stress at the instability initiation in double-network hydrogel (Na et al., 2006). After the necking, the thick and thin states coexist in the bar at a constant nominal stress, with the thin state growing at the expense of the thick state (Fig. 11(a) and (b)). The value of the nominal stress for the transition is determined by Maxwell's rule as shown in Fig. 10(a). Once all the thick state has transited into the thin state (e.g. $l/L=2.7$), the nominal stress increases rapidly with the stretch, due to the stiffening of the longer-chain network (Fig. 11(a) and (b)). If the effective stretch is reduced, the bar deforms homogeneously back to its original shape. The necking instability does not occur during the unloading process, because the shorter-chain network has been damaged. The energy dissipated during the damage of the shorter-chain

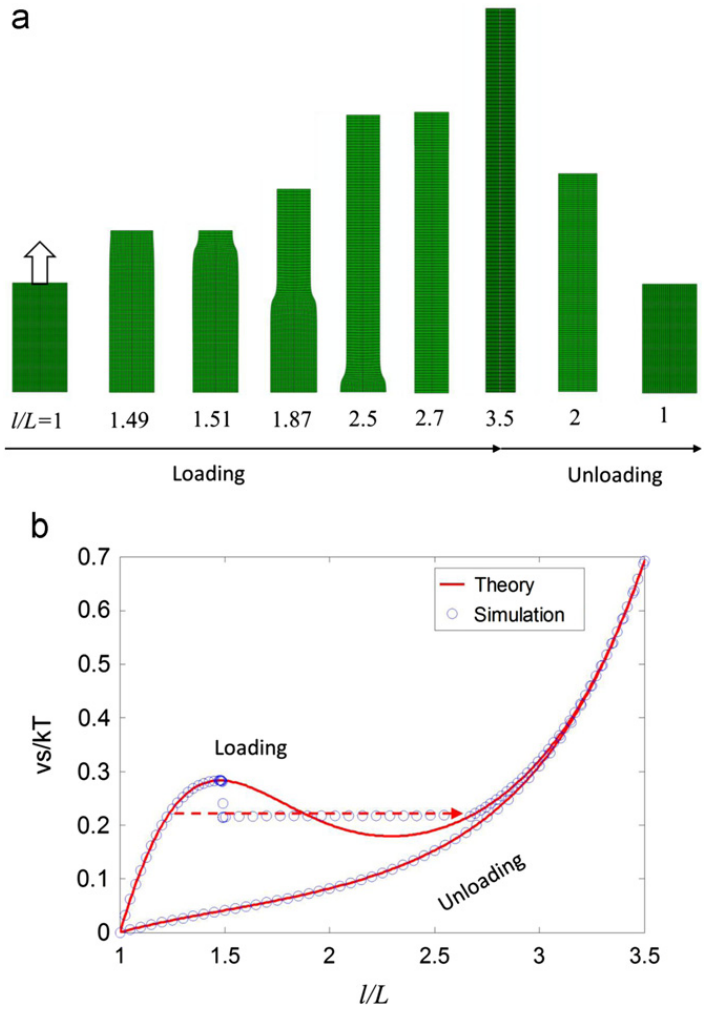

Fig. 11. Numerical simulation of the initiation and propagation of necking instability in a bar of a double-network hydrogel (a) and the evolution of nominal stress in the bar (b).

network is reflected by the hysteresis loop on the stress-stretch curve in Fig. 11(b). Further, if the deformed the bar is stretched again, no necking instability occurs either. The theoretical and numerical results in Fig. 11(a) and (b) are consistent with the experimental observations by Na et al. (2006).

5. Conclusion

A mechanistically motivated model has been developed to account for the large deformation and damage of interpenetrating polymer networks. By integrating the interpenetrating network model and the network alteration theory, our model is capable of quantitatively characterizing the Mullins effect and necking instability experimentally observed in double-network hydrogels. The interpenetration of one network stretches polymer chains in the other network and reduces its chain density, significantly affecting the initial modulus, stiffening and damage properties of the resultant IPNs. The characters of stiffening and subsequent damage of one network determine the special Mullins effect of double-network hydrogels. The necking instability of double-network hydrogels requires both the damage-induced softening of one network and the polymer-chain stiffening of the other network. Our model is further implemented into finite-element software to simulate the initiation and propagation of necking instability in double-network hydrogels. The theoretical and numerical results are compared with experimental data from multiple compressive and tensile tests. We note that Wang and Hong (2011) reported a phenomenological model for double-network hydrogels, when the current paper was under review.

Acknowledgment

Funding for this research was provided by the NSF's Research Triangle MRSEC (DMR-1121107) and Pratt School of Engineering at Duke University. The author acknowledges J.P. Gong's comments on a draft of the paper, and the helpful discussions from J.P. Gong, Z.G. Suo, C. Creton, and W. Hong.

References

An, Y.H., Solis, F.J., Jiang, H.Q., 2010. A thermodynamic model of physical gels. J. Mech. Phys. Solids 58, 2083–2099.
Arruda, E.M., Boyce, M.C., 1993. A 3-dimensional constitutive model for the large stretch behavior of rubber elastic-materials. J. Mech. Phys. Solids 41, 389–412.
Bergstrom, J.S., Boyce, M.C., 1999. Mechanical behavior of particle filled elastomers. Rubber Chem. Technol. 72, 633–656.
Berry, J.P., Scanlan, J., Watson, W.F., 1956. Cross-link formation in stretched rubber networks. Trans. Faraday Soc. 52, 1137–1151.
Blanchard, A.F., Parkinson, D., 1952. Breakage of carbon-rubber networks by applied stress. Ind. Eng. Chem. 44, 799–812.
Boyce, M.C., Arruda, E.M., 2000. Constitutive models of rubber elasticity: a review. Rubber Chem. Technol. 73, 504–523.
Boyce, M.C., Arruda, E.M., 2001. Swelling and mechanical stretching of elastomeric materials. Math. Mech. Solids 6, 641–659.
Brochu, P., Yuan, W., Zhang, H., Pei, Q.B., Asme, 2009. Dielectric elastomers for direct wind-to-electricity power generation. SMASIS 1, 197–204.
Brown, H.R., 2007. A model of the fracture of double network gels. Macromolecules 40, 3815–3818.
Chagnon, G., Verron, E., Marckmann, G., Gornet, L., 2006. Development of new constitutive equations for the Mullins effect in rubber using the network alteration theory. Int. J. Solids Struct. 43, 6817–6831.
Chater, E., Hutchinson, J.W., 1984. On the propagation of bulges and buckles. J. Appl. Mech.—Trans. ASME 51, 269–277.
Dorfmann, A., Ogden, R.W., 2003. A pseudo-elastic model for loading, partial unloading and reloading of particle-reinforced rubber. Int. J. Solids Struct. 40, 2699–2714.
Fleck, N.A., Muller, G.M., Ashby, M.F., Hutchinson, J.W., 1994. Strain gradient plasticity—theory and experiment. Acta Metall. Mater. 42, 475–487.
Flory, P.J., 1960. Elasticity of polymer networks cross-linked in states of strain. Trans. Faraday Soc. 56, 722–743.
Flory, P.J., Rehner, J., 1943a. Statistical mechanics of cross-linked polymer networks I. Rubberlike elasticity. J. Chem. Phys. 11, 512–520.
Flory, P.J., Rehner, J., 1943b. Statistical mechanics of cross-linked polymer networks II Swelling. J. Chem. Phys. 11, 521–526.
Gong, J.P., Katsuyama, Y., Kurokawa, T., Osada, Y., 2003. Double-network hydrogels with extremely high mechanical strength. Adv. Mater. 15, 1155–1158.
Goulbourne, N.C., 2011. A constitutive model of polyacrylate interpenetrating polymer networks for dielectric elastomers. Int. J. Solids Struct. 48, 1085–1091.
Govindjee, S., Simo, J., 1991. A micro-mechanically based continuum damage model for carbon black-filled rubbers incorporating mullins effect. J. Mech. Phys. Solids 39, 87–112.
Ha, S.M., Yuan, W., Pei, Q.B., Pelrine, R., Stanford, S., 2006. Interpenetrating polymer networks for high-performance electroelastomer artificial muscles. Adv. Mater. 18 887.
Halls, J.J.M., Walsh, C.A., Greenham, N.C., Marseglia, E.A., Friend, R.H., Moratti, S.C., Holmes, A.B., 1995. Efficient photodiodes from interpenetrating polymer networks. Nature 376, 498–500.
Hong, W., Zhao, X.H., Zhou, J.X., Suo, Z.G., 2008. A theory of coupled diffusion and large deformation in polymeric gels. J. Mech. Phys. Solids 56, 1779–1793.
Hutchinson, J.W., Neale, K.W., 1981. In: Carlson, D.E., Shield, R.T. (Eds.), Finite Strain J2 Deformation Theory, Martinus Nijhoff Publishers, Netherlands, pp. 238–247.
Johnson, M.A., Beatty, M.F., 1993. A constitutive equation for the mullins effect in stress controlled uniaxial extension experiments. Continuum Mech. Thermodyn. 5, 301–318.
Koh, S.J.A., Zhao, X.H., Suo, Z.G., 2009. Maximal energy that can be converted by a dielectric elastomer generator. Appl. Phys. Lett. 94, 262902.
Kuhn, W., Grun, F., 1942. Relations between elastic constants and the strain birefringence of high-elastic substances. Kolloid Zh. 101, 248–271.
Lake, G.J., Thomas, A.G., 1967. Strength of highly elastic materials. Proc. R. Soc. London Ser. A—Math. Phys. Sci. 300 108.
Lion, A., 1996. A constitutive model for carbon black filled rubber: experimental investigations and mathematical representation. Continuum Mech. Thermodyn. 8, 153–169.
Ma, W.L., Yang, C.Y., Gong, X., Lee, K., Heeger, A.J., 2005. Thermally stable, efficient polymer solar cells with nanoscale control of the interpenetrating network morphology. Adv. Funct. Mater. 15, 1617–1622.
Marckmann, G., Verron, E., Gornet, L., Chagnon, G., Charrier, P., Fort, P., 2002. A theory of network alteration for the Mullins effect. J. Mech. Phys. Solids 50, 2011–2028.
Mark, J.E., 1999. Improved elastomers through control of network chain-length distributions. Rubber Chem. Technol. 72, 465–483.

McMeeking, R.M., Evans, A.G., 1982. Mechanics of transformation-toughening in brittle materials. J. Am. Ceram. Soc. 65, 242–246.
Miehe, C., 1995. Discontinuous and continuous damage evolution in Ogden-type large-strain elastic-materials. Eur. J. Mech. A—Solids 14, 697–720.
Mullins, L., Tobin, N.R., 1965. Stress softening in rubber vulcanizates. I. Use of a strain amplification factor to describe elastic behavior of filler-reinforced vulcanized rubber. J. Appl. Polym. Sci. 9 2993.
Na, Y.H., Tanaka, Y., Kawauchi, Y., Furukawa, H., Sumiyoshi, T., Gong, J.P., Osada, Y., 2006. Necking phenomenon of double-network gels. Macromolecules 39, 4641–4645.
Nakajima, T., Furukawa, H., Tanaka, Y., Kurokawa, T., Osada, Y., Gong, J.P., 2009. True chemical structure of double network hydrogels. Macromolecules 42, 2184–2189.
Qi, H.J., Boyce, M.C., 2004. Constitutive model for stretch-induced softening of the stretch–stress behavior of elastomeric materials. J. Mech. Phys. Solids 52, 2187–2205.
Risbud, M.V., Hardikar, A.A., Bhat, S.V., Bhonde, R.R., 2000. pH-sensitive freeze-dried chitosan-polyvinyl pyrrolidone hydrogels as controlled release system for antibiotic delivery. J. Controlled Release 68, 23–30.
Rubinstein, M., Colby, R.H., 2003. Polymer Physics. Oxford University Press.
Sperling, L.H., Mishra, V., 1996. The current status of interpenetrating polymer networks. Polym. Adv. Technol. 7, 197–208.
Sun, J.-Y., Zhao, X., Illeperuma, W.R.K., Oh, K.H., Mooney, D.J., Vlassak, J.J., Suo, Z., 2011. PAAm-alginate interpenetrating network hydrogel with extremely high toughness. Unpublished.
Suo, Z.G., Zhu, J., 2009. Dielectric elastomers of interpenetrating networks. Appl. Phys. Lett. 95, 232909.
Tanaka, Y., 2007. A local damage model for anomalous high toughness of double-network gels. EPL 78, 56005.
Tanaka, Y., Kuwabara, R., Na, Y.H., Kurokawa, T., Gong, J.P., Osada, Y., 2005. Determination of fracture energy of high strength double network hydrogels. J. Phys. Chem. B 109, 11559–11562.
Treloar, L.R.G., Riding, G., 1979. Non-Gaussian theory for rubber in biaxial strain. 1. Mechanical-properties. Proc. R. Soc. London Ser. A—Math. Phys. Eng. Sci. 369, 261–280.
von Lockette, P.R., Arruda, E.M., Wang, Y., 2002. Mesoscale modeling of bimodal elastomer networks: constitutive and optical theories and results. Macromolecules 35, 7100–7109.
Wang, M.C., Guth, E., 1952. Statistical theory of networks of non-Gaussian flexible chains. J. Chem. Phys. 20, 1144–1157.
Wang, X., Hong, W., 2011. Pseudo-elasticity of a double network gel. Soft Matter 7, 8576–8581.
Webber, R.E., Creton, C., Brown, H.R., Gong, J.P., 2007. Large strain hysteresis and mullins effect of tough double-network hydrogels. Macromolecules 40, 2919–2927.
Yasuda, K., Kitamura, N., Gong, J.P., Arakaki, K., Kwon, H.J., Onodera, S., Chen, Y.M., Kurokawa, T., Kanaya, F., Ohmiya, Y., Osada, Y., 2009. A novel double-network hydrogel induces spontaneous articular cartilage regeneration in vivo in a large osteochondral defect. Macromol. Biosci. 9, 307–316.
Yu, Q.M., Tanaka, Y., Furukawa, H., Kurokawa, T., Gong, J.P., 2009. Direct observation of damage zone around crack tips in double-network gels. Macromolecules 42, 3852–3855.
Zhao, X.H., Hong, W., Suo, Z.G., 2007. Electromechanical hysteresis and coexistent states in dielectric elastomers. Phys. Rev. B 76, 134113.
Zhao, X.H., Suo, Z.G., 2007. Method to analyze electromechanical stability of dielectric elastomers. Appl. Phys. Lett. 91, 061921.
Zhao, X.H., Suo, Z.G., 2010. Theory of dielectric elastomers capable of giant deformation of actuation. Phys. Rev. Lett. 104, 178302.